Electrochimica Acta 55 (2010) 6010–6014

Contents lists available at ScienceDirect

Electrochimica Acta

journal homepage: www.elsevier.com/locate/electacta

Electrochemical treatment of tumors using a one-probe two-electrode device

N. Olaiz [a], F. Maglietti [a], C. Suárez [a], F.V. Molina [b], D. Miklavcic [c], L. Mir [d], G. Marshall [a,*]

[a] Laboratorio de Sistemas Complejos, Departamento de Computacion, Facultad de Ciencias Exactas y Naturales, Universidad de Buenos Aires, Ciudad Universitaria, Pabellon I, C1428EGA Buenos Aires, Argentina
[b] INQUIMAE, Facultad de Ciencias Exactas y Naturales, Universidad de Buenos Aires, C1428EGA Buenos Aires, Argentina
[c] Faculty of Electrical Engineering, University of Ljubljana, Tržaška 25, SI-1000 Ljubljana, Slovenia
[d] Institut Gustave-Roussy, Univ Paris-Sud, Paris, France

ARTICLE INFO

Article history:
Received 7 March 2010
Received in revised form 10 May 2010
Accepted 15 May 2010
Available online 24 May 2010

Keywords:
Tumors
Electrochemical treatment
Electrochemotherapy
pH front tracking
In vitro models

ABSTRACT

We have recently shown that in the classical electrochemical treatment (EChT) of tumors, i.e., the passage of a direct electric current through two electrodes inserted locally in the tumor tissue, from an initial uniform condition two pH fronts evolve, expanding towards each other, inducing extreme pH changes and tumor destruction, mainly by necrosis. Here we extend these results introducing a one-probe two-electrode device (OPTED) containing the cathode and the anode very close to each other (1 mm). Experiments show that upon application of the OPTED-EChT, two half-spherical pH fronts, one basic and the other acid (from cathode and anode, respectively), expand towards the periphery configuring a distorted full sphere. Tracking of the pH front advance reveals a time scaling close to $t^{1/2}$, signature of a diffusion-controlled process. An analytic model presented allows the estimation of the time needed for total tumor destruction with a minimum compromise of healthy tissue. Main advantages of the OPTED are the insertion of one applicator rather than two or more (thus minimizing tissue intrusion, for instance, in the nervous system), the ability to reach tumors beyond capabilities of conventional surgery and the minimization of electric current circulation through the treated organ. We propose here this new design which could have significant implications in EChT optimal operative conditions, in particular, in the way in which the evolving pH spherical fronts can cover and destroy a cancer cell spherical casket.

1. Introduction

The electrochemical treatment (EChT) or electrotherapy of tumors consists in the passage of a direct electric current through two or more electrodes inserted locally in the tumor tissue [1,2]. Tissue destruction has been reported in a wide range of solid tumors at the clinical level, especially in skin, lung, liver, pancreas and breast malignancies [3–5]. Also, the use of direct electric currents in tumor treatment in combination with other approaches has been explored [6–9]. Clinical experience has shown that EChT is a relatively low cost, safe, minimally traumatic and effective cancer treatment option, specially indicated in patients none suited for surgery or tumors irresponsive to radio or chemotherapy. Electrochemical reactions in EChT induce extreme pH changes and, consequently, protein electrodenaturation fronts intimately related to tumor destruction. Since necrotic areas correlate well with those covered by alkaline and acid fronts advance, pH front tracking can be used to predict the extent of tumor destruction and thus EChT effectiveness [10–12]. A somehow related method allowing rapid visualization of the entire pH distribution by using laser confocal scanning microscopy coupled to microelectrochemistry was recently presented in Refs. [13,14].

In Ref. [15] we have shown that under EChT modeling with two well separated platinum tip electrodes inserted into a collagen gel, from an initial condition with almost neutral pH, extreme cathodic alkaline and anodic acidic fronts evolve moving towards each other, leaving the possible existence of a biological pH region between them; towards the periphery, the pH decays to its neutral values. Moreover, pH front tracking unveils a time scaling close to $t^{1/2}$, signature of a diffusion-controlled process. These results were extended in Ref. [16] where more realistic simulations were presented. In Ref. [17] we introduced a new in vitro EChT collagen-macronutrient gel (CMG) model to study protein electrodenaturation fronts as a means of assessing EChT effectiveness. Here again, electrodenaturation front tracking reveals a diffusion-controlled process.

In the classical EChT method, the distance between the two electrodes is in general in the order of centimeters, the reason being that is generally believed that there exists an optimal distance between the electrodes and that if the anode and cathode are placed too close to each other, chemical reactions between the different electrode reaction products are possible. Moreover, the

* Corresponding author. Tel.: +54 11 4576 3390x709; fax: +54 11 4576 3359.
E-mail address: marshallg@arnet.com.ar (G. Marshall).

0013-4686/$ – see front matter © 2010 Elsevier Ltd. All rights reserved.
doi:10.1016/j.electacta.2010.05.057

effect of clinical treatment, using electrodes placed close together, has not been as good as in those cases where the separation was large enough that their destruction zones did not overlap [18]. At variance with this belief, here we introduce a one-probe two-electrode device (OPTED) containing the cathode and the anode very close to each other (1 mm), that it is shown to have many advantages over classical electrode separation. Since the effects of the exposure of a 3D gel model during OPTED-EChT can be assessed by the area covered by pH fronts, here we perform pH front tracking by means of pH indicators color change.

The aim of this work is to introduce the OPTED device in combination with a 3D gel model for studying pH front evolution during EChT treatment. The rationale is that effects of the exposure of a tumor to OPTED-EChT therapy can be assessed using a 3D gel model through the volume swept by the pH fronts. The ultimate goal is the OPTED-EChT optimization in clinical applications. The main advantages of the use of this new design over classical EChT applications are that current circulation is limited to a very small region between electrodes (relevant for treatment in cardiac or nervous tissues) and the insertion of only one catheter rather than two or more, minimizes tissue intrusion. The plan of the paper is the following: Section 2 describes materials and methods, Section 3 presents results and discussions and finally, Section 4, some general conclusions.

2. Experimental

The experimental setup is shown in Fig. 1. The gel used consisted of 1% agar-agar in distilled water, with NaCl at physiological concentration (0.16 mol/dm^3), phenolphthalein ($C_{20}H_{14}O_4$, transition pH range 8.0–9.6) and methyl red ($C_{15}H_{16}N_3O_2Cl$, transition pH range 4.8–6.2) as basic and acid indicators, respectively. The solution was placed in a transparent plastic cube (2.3 cm × 2.3 cm × 1.8 cm, 3D model) and allowed to gel. Two platinum needle electrodes (electrically insulated except at the tip) were inserted in the center of the gel with a separation of 1 mm between each other, and an exposed area of 1.5×10^{-3} cm^2, each. Total diameter of the OPTED is of 5 mm. All experiments were conducted at room temperature with no significant changes observed during the process.

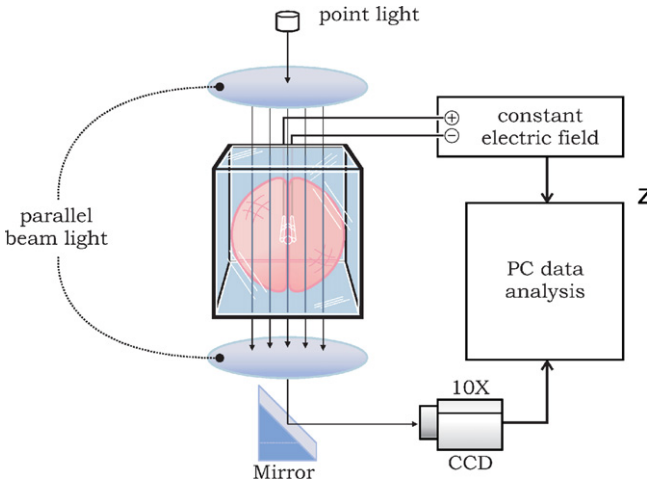

Fig. 1. Experimental setup used for image acquisition and coordinate system.

Visual front tracking of the pH fronts emerging from the electrodes was obtained by an optical absorption technique. Illumination was achieved by a high intensity white led with emission wavelengths near the maximum absorption of the indicators basic and acid forms (374 nm for phenolphthalein and 520 nm for methyl red, respectively). Video images were obtained with a CCD Sony XC-HR50. ImageJ graphic package (http://rsbweb.nih.gov/ij/) was used for image capturing and processing. Front position measurements are accurate to ±0.3 mm for the acid front and 0.1 mm for the alkaline one. A constant direct electric current ranging between 2 and 10 mA was applied (power supply: Consort E835, Belgium). Electric current and voltage were continuously monitored by a standard

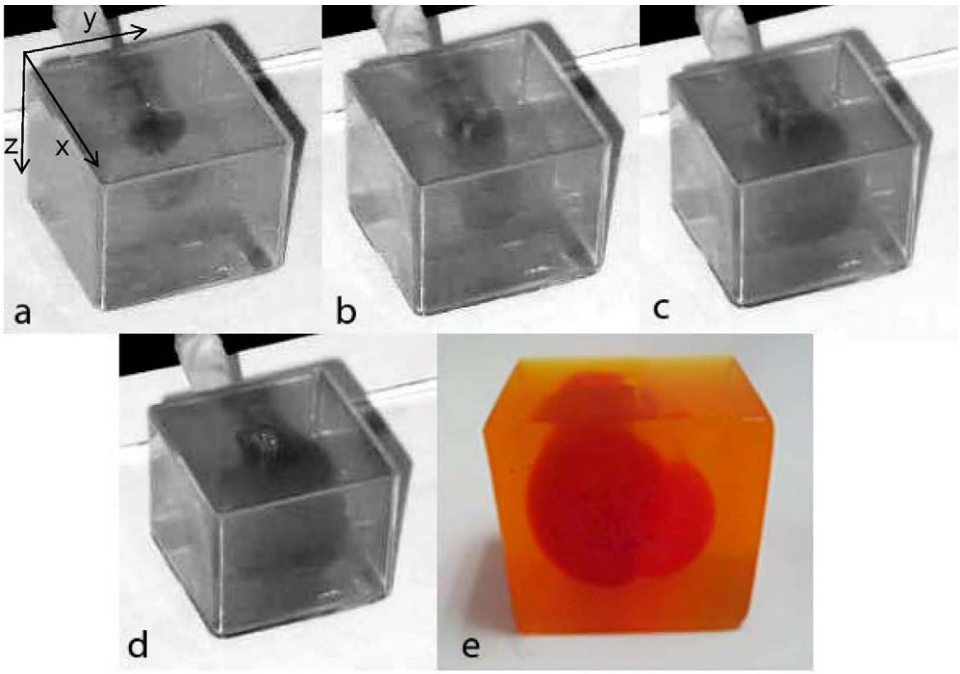

Fig. 2. Time (s) sequence of digital images showing the effects of the exposure of a 3D gel model during OPTED-EChT with a constant current of 10 mA. (a) 5 s, (b) 70 s, (c) 350 s, (d) 530 s and (e) 1200 s. Growth of pH front halo around electrodes is clearly seen. (e) Final state after the EChT where both anodic and cathodic hemispheres (left and right side, respectively) can be observed.

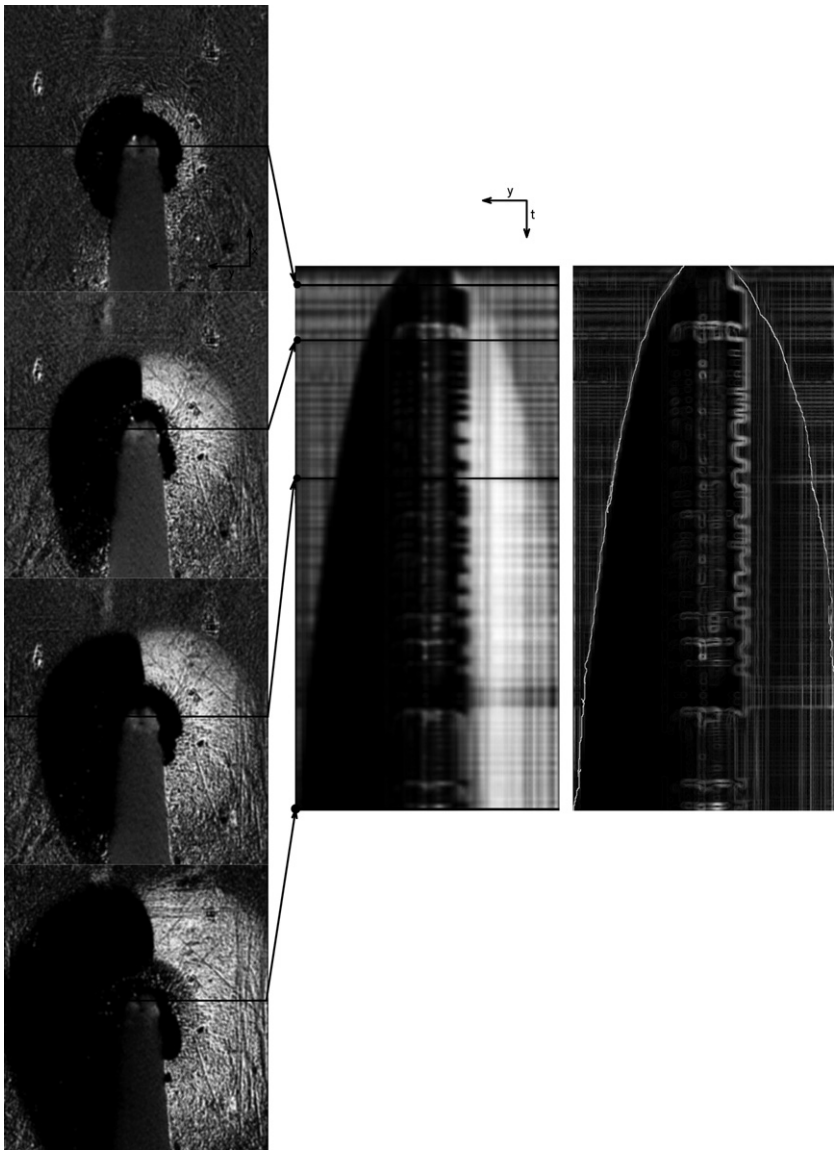

Fig. 3. Time (s) sequence of digital images (taken from above) showing the evolution of the acid and basic pH fronts in a 3D gel model during OPTED-EChT with a constant current of 4 mA. Left pane, from top to down: (a) 100 s, (b) 300 s, (c) 700 s and (d) 1200 s. Center pane: reslice from the sequence of images. Lines joining left and center panes indicate where the left image is located in the stack. Right pane: calculated trajectory of both pH fronts.

multimeter (20 s sampling). The applied voltage was almost constant during the course of the experiments, ranging from 3.9 V at 2 mA to 5.1 V at 10 mA.

3. Results and discussion

Effects of the exposure of a 3D gel model during OPTED-EChT with a constant current of 10 mA are shown in Fig. 2 comprising a time sequence of digital images. The sequence unveils the gradual appearance of hemisphere-like shape halos or a quasi-spherical pH fronts around both electrodes, causing a change from the initially homogeneous color of the medium. Fig. 2e is reproduced in color (for the online version) to show more clearly the actual front evolution. Cathodic and anodic pH fronts evolve towards a well-defined and stable shape: at a central zone both fronts encounter and collide and remain stand still due to neutralization; towards the periphery, both fronts evolve as hemisphere-like growing halos. At this constant current value, the final acidic hemisphere is larger than the basic one, evidencing larger proton front velocity. This could be due to the larger diffusion coefficient of this ion relative to that of hydroxides. Nevertheless, the final area reached by the OPTED-EChT process can be assimilated to a quasi-full sphere.

The 2D space and time representation of the OPTED-EChT experiment showing the evolution of the acid and basic pH fronts are depicted in Fig. 3 (data taken from a similar experiment as that in Fig. 2). The left pane is a sequence of four snapshots at different times extracted from a video of 1200 s duration in which the camera is viewing the process from above. Acid and basic pH fronts are represented by bright and dark pixels, respectively. The central pane is a reslice, constructed from digital gray scales made from a sequence of images such as those shown in the left figure. Measurements made each second are averaged over 1% of the cell width (direction parallel to the *y* axis) to reduce each image to a line. Then these lines are stacked to yield the space-time image spanning the duration of the experiment (1200 s). The right pane depicts the trajectory of both fronts and is the result of a border detection algorithm applied to the central figure.

Fig. 4 presents the plots of the tracking of the experimental values of the cathodic (OH^-) and anodic (H^+) pH fronts for different constant current values. Black and gray symbols indicate basic and

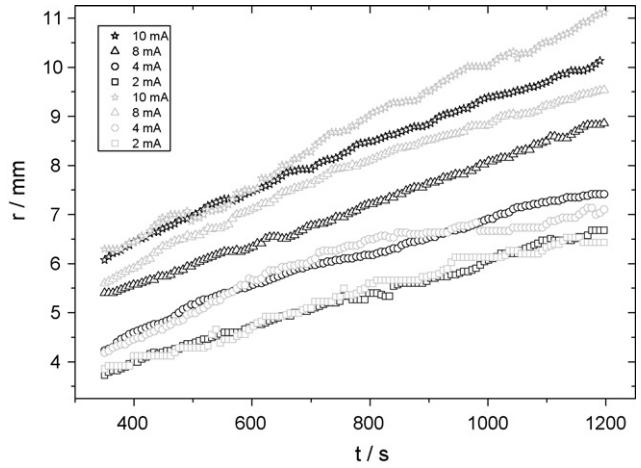

Fig. 4. Distance from electrode (mm) vs. time (s) of acid and basic pH front advance at different electric current intensities (2, 4, 8 and 10 mA) during exposure of the 3D gel model to an OPTED-EChT. Anodic and cathodic fronts are shown as gray and black symbols, respectively.

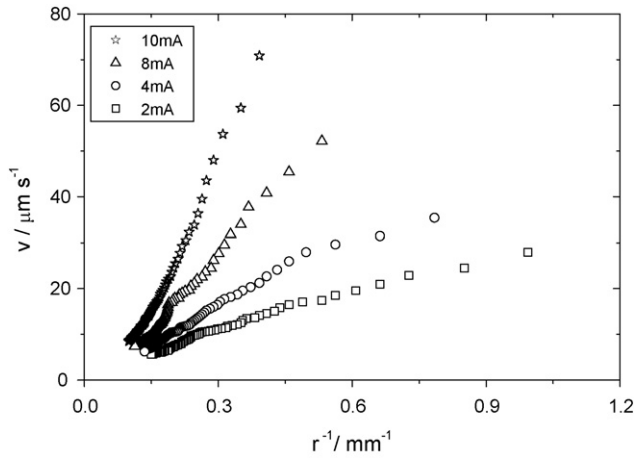

Fig. 6. Velocity of the cathodic pH front v (μm/s) vs. the inverse of the distance r^{-1} (mm^{-1}) at different electric current intensities (2, 4, 8 and 10 mA), in the exposure of the 3D gel model during OPTED-EChT.

acid pH fronts, respectively (this graph is based upon the trajectories obtained from Fig. 3, right image). The results for anodic and acid fronts are rather similar though the acid front advances with higher speed. We attribute this fact to the H^+ diffusion coefficient being higher than that of OH^-, as it is well known. However, the ratio of the two speeds is lower than the ratio $D_H/D_{OH} \approx 1.7$; this difference is attributed to the evolution of Cl_2 on the anode, as it is well known [18], thus resulting in a lower efficiency for H^+ production compared with that of OH^-. It is worth remarking that the anodic front measurements are more difficult because this front is not well defined in the images and at long times the fronts pass beyond the image borders. As a consequence, the H^+ front positions are affected by uncertainties somewhat higher than those of the cathodic OH^- front. Nevertheless, the higher speed of the H^+ front is observed, particularly at higher current values.

Fig. 5 shows the plots of the tracking of the experimental values of the cathodic (OH^-) front for different constant current values (in symbols). The inset shows a log–log plot of the data corresponding to 10 mA. A good fitting is obtained with $r = Kt^m$ with $m = 0.45$, value close to 1/2, strongly suggesting a diffusion-controlled process. For such a process to be diffusion-controlled, the space-time dependence of the concentration of H^+ and OH^- ions in the anodic and cathodic hemispheres, respectively, can be rationalized on the

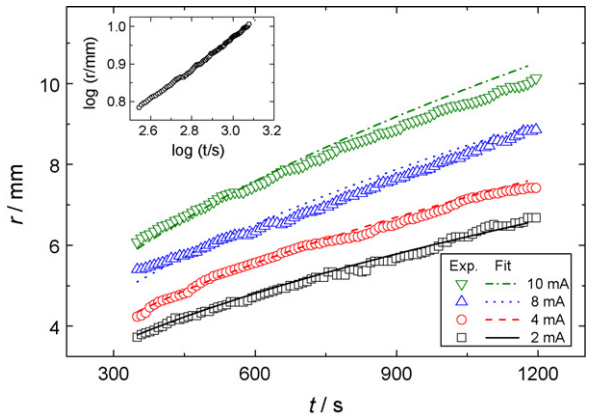

Fig. 5. Distance from electrode r (mm) vs. time t (s) for cathodic pH front advance at different electric current intensities (2, 4, 8 and 10 mA), in the exposure of the 3D gel model during OPTED-EChT. Experimental curves in symbols, theoretical curve from Eq. (1) in thin lines.

basis of Fick's law with spherical boundary conditions resulting, for the cathodic front, in the well known expression [19]:

$$C_{OH} = C^0_{OH} + \frac{i}{nFAD^{1/2}}\frac{r_0}{r} \times \left\{ 2\left(\frac{t}{\pi}\right)^{1/2} \exp\left[-\frac{(r-r_0)^2}{4Dt}\right] - \frac{(r-r_0)}{D^{1/2}} \operatorname{erfc}\left[\frac{r-r_0}{2(Dt)^{1/2}}\right] \right\} \quad (1)$$

here C_{OH} is the hydroxide concentration (in the cathodic pH front), C^0_{OH} the hydroxide concentration at a spatial point far enough from electrode, i the electric current intensity, r_0 the radius of a virtual spherical electrode, r the distance from the electrode, n the number of electrons involved, F the Faraday's constant, A the electrode conducting area, D the hydroxide ion diffusion constant and t the time elapsed. For the anodic front (H^+ front) the same equation applies changing only the C, C^0 and D values for those corresponding to protons.

It has been assumed here that the reactant, water, has a constant concentration through the experiment. Fig. 5 also shows the theoretical curves (thin lines) from Eq. (1) for comparison with the experimental data. The former are obtained by assuming that the front is detected when C_{OH} reaches a predefined value ($C_{OH} = 10^{-5}$ M, i.e., pH 9.0) and solving Eq. (1) for r at each t value. Here, the electrode conducting area was fitted for each value of the electric current (2 mA: 27.3 mm^2, 4 mA: 8.6 mm^2, 8 mA: 1.17 mm^2, 10 mA: 0.052 mm^2). A good correlation is obtained if data at earlier times is discarded, indicating that at longer distances from the electrode, transport is mainly governed by diffusion which confirms our previous suggestion. At closer distances, the process is more complex and not well described by diffusion alone; most probably convection or electroosmosis must be taken into consideration. More research is in course to clarify this point.

Fig. 6 shows experimental curves of cathodic pH front velocity vs. the inverse of the distance to the electrode, for different electric currents. Results show that at an earlier time pH front velocities are larger and appear to scale linearly with the distance to the electrode. Thus, taking the pH front velocity as a linear function of the inverse of r, the time needed for tumor destruction without compromising healthy tissue can be estimated knowing the geometry of the problem.

The OPTED electrode configuration implies that, for clinical applications, circulation of current through the treated organ is negligible as it is limited to a very small area between electrodes. This is especially important if treatment must be applied in cardiac

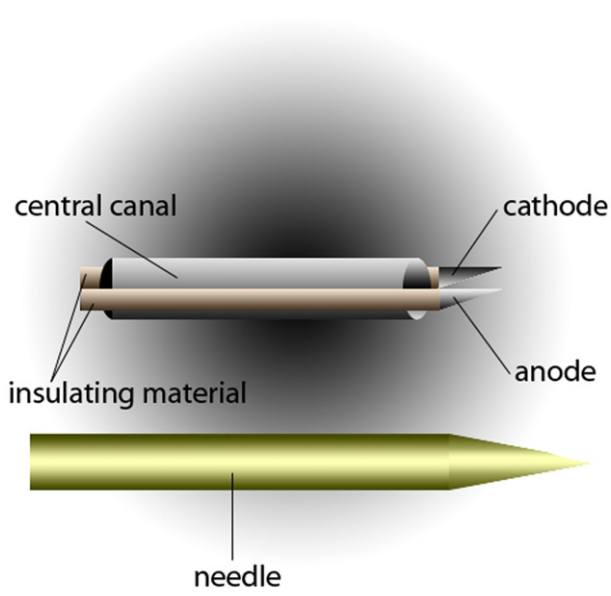

Fig. 7. Schematic design of the possible adaptation of the OPTED for needle insertion in the central canal. This would allow a biopsy, adjuvant injection or necrotic tissue removal, to be associated with the EChT procedure.

or nervous tissues. Other advantages of this new application design are the insertion of only one catheter rather than two or more (thus minimizing tissue intrusion) and eliminating the possible existence of a physiological pH remnant area between electrodes. As other non-selective therapies, the OPTED-EChT can in principle eliminate all kind of tumors. However, it does not have the severe toxicity limitations presented by chemo or radiotherapy. The maximum volume that can be covered with this technique would depend on two factors: first is the dose (i.e., charge) delivered in the treatment, and second the exhaustion of water in the vicinity of the OPTED, leading to the occurrence of side reactions and a decrease in the efficiency of H^+ and OH^- production, in turn causing the pH fronts to be retarded or fully detained.

Due to the possibility of reaching tumors beyond conventional surgery, the OPTED can be used to access deep or difficult-to-reach regions of the human body using the already known ways of entry and techniques of endoscopy, biopsy or catheterism. At the clinical level, there is a pilot study on the use of EChT as a palliative treatment of malignant dysphagia that uses a somehow similar type of electrode introduced endoscopically through the esophagus [20]. The OPTED-EChT may have also some other advantages over other catheter ablation techniques in common use in clinical medicine, as radiofrequency ablation used in cardiac arrhythmias. By this technique, tissue temperature may remain high for many seconds despite cessation of energy delivery, producing undesired ablation of treated structures [21]. On the contrary, there is no heat production with the OPTED-EChT, minimizing uncontrolled tissue destruction in the periphery of the treated area.

The OPTED can eventually be adapted to simultaneously inject a chemical agent and/or remove necrotic tissue in association with the EChT procedure. This could be achieved by inserting a needle inside the central canal between electrodes (as shown in Fig. 7). Indeed, it has been described the convenience of applying sodium chloride in conjunction with the EChT for improving the electric current circulation [22]. The device may also have potential advantages in the application of electrochemotherapy, other electric current-based therapy where electric pulses are combined with chemotherapeutic agents to improve their cellular uptake by the induction of electroporation [23]. Finally, the OPTED can also be adapted to any of the existing methods of biopsy (including stereotactic biopsy in the central nervous system).

4. Conclusions

We introduced a one-probe two-electrode device (OPTED) containing the cathode and the anode very close to each other (1 mm). We showed that upon application of the OPTED-EChT to an in vitro 3D gel model, from an initial uniform condition, two half-spherical pH fronts emerge, one basic the other acid (from cathode and anode, respectively), expanding towards the periphery conforming a quasi-full sphere. pH front tracking reveals a time scaling close to $t^{1/2}$, signature of a diffusion-controlled process, thus allowing the prediction of the necessary time needed for total tumor destruction with minimum compromise of healthy tissue. In contrast to the traditional EChT electrode setup, OPTED-EChT has some convenient advantages, as the insertion of only one applicator, the possibility of reaching tumors beyond capabilities of conventional surgery and the minimization of electric current circulation through the treated organ. We hope this new design could have significant implications in EChT optimal operative conditions, in particular, in the way in which the evolving pH spherical fronts can cover and destroy a cancer cell spherical casket.

Acknowledgements

N. Olaiz has a fellowship from Consejo Nacional de Investigaciones Cientificas y Tecnicas (CONICET), C. Suarez, F. Molina and G. Marshall are researchers at CONICET. This work is supported by grants from CONICET (PIP 5756/05), Universidad de Buenos Aires (UBACyT X132/08) and Argentine-Slovenia Scientific Collaboration Project (SLO0802/2008).

References

[1] B. Nordenstrom, Am. J. Clin. Oncol.: Cancer Clin. Trials 12 (1989) 530.
[2] E. Nilsson, H. von Euler, J. Berendson, A. Thorne, P. Wersall, I. Naslund, A. Lagerstedt, K. Narfstrom, J. Olsson, Bioelectrochemistry 51 (2000) 1.
[3] Y. Xin, J. IABC 1 (2002) 24.
[4] A. Plesnicar, D. Sersa, L. Vodovnik, B. Jancar, L. Zaletel-Kragelj, S. Plesnicar, Eur. J. Surg. Suppl. 574 (1994) 45.
[5] M. Tello, L. Oliveira, O. Parise, A. Buzaid, R. Oliveira, R. Zanella, A. Cardona, Proceedings of the 29th Annual International Conference of the IEEE EMBS, 2007, p. 3524.
[6] D. Miklavciic, D. An, J. Belehradek, L. Mir, Eur. Cytokine Netw. 8 (1997) 275.
[7] Y. Xin, D. Liu, G. Ghen, Y. Guo, F. Zhao, J. IABC 1 (2002) 45.
[8] C. Dobbins, C. Brennan, S. Wemyss-Holden, J. Cockburn, G. Maddern, ANZ J. Surg. 78 (2008) 568.
[9] A. Mikhailovskaya, M. Kaplan, R. Brodskij, L. Bandurko, Bull. Exp. Biol. Med. 147 (2009) 88.
[10] B. Tang, L. Li, Z. Jiang, Y. Luan, D. Li, W. Zhang, E. Reed, Q. Li, Int. J. Oncol. 26 (2005) 703.
[11] J. Finch, B. Fosh, A. Anthony, E. Slimani, M. Texler, D. Berry, A. Dennison, G. Maddern, Clin. Sci. (Lond) 102 (2002) 389.
[12] M. Avramov Ivic, S. Petrovic, P. Zivkovic, N. Nikolic, K. Popov, J. Electroanal. Chem. 549 (2003) 129.
[13] J. Grime, M. Edwards, N. Rudd, P. Unwin, PNAS 105 (2008) 14277.
[14] J. Zhang, D. Burt, A. Whitworth, D. Mandler, P. Unwin, Phys. Chem. Chem. Phys. 11 (2009) 3490.
[15] L. Colombo, G. Gonzalez, G. Marshall, F. Molina, A. Soba, C. Suarez, P. Turjanski, Bioelectrochemistry 71 (2007) 223.
[16] P. Turjanski, N. Olaiz, P. Abou-Adal, C. Suarez, M. Risk, G. Marshall, Electrochim. Acta 54 (2009) 6199.
[17] N. Olaiz, C. Suarez, M. Risk, F. Molina, G. Marshall, Electrochem. Commun. (2009), doi:10.1016/j.elecom.2009.10.044.
[18] E. Nilsson, J. Berendson, E. Fontes, J. Electroanal. Chem. 460 (1999) 88.
[19] D.D. Macdonald, Transient Techniques in Electrochemistry, Plenum Press, New York, 1977, Chap. 5.
[20] M. Wojcicki, R. Kostyrka, B. Kaczmarek, J. Kordowski, M. Romanowski, M. Kaminski, J. Klonek, S. Zielinski, Hepatogastroenterology 46 (1999) 278.
[21] A. Fauci, E. Braunwald, D. Kasper, S. Hauser, D. Longo, J. Jameson, J. Loscalzo, in: T. M.-H. Companies (Ed.), Harrison's Principles of Internal Medicine, vol. II, 17th edition, 2008.
[22] X. Lin, C. Jen, C. Chou, C. Chou, M. Sung, T. Chou, Dig. Dis. Sci. 45 (2000) 509.
[23] L. Mir, Eur. J. Cancer Suppl. 4 (2006) 38.